Check for updates

Influence of *para*-substitution on the polymerisation kinetics of 2-phenyl-2-oxazolines†

Chloe M. Shilling, Lloyd A. Shaw, [ID] Juan A. Aguilar, [ID] William D. G. Brittain [ID] * and Clare S. Mahon [ID] *

A series of cationic ring opening polymerisations (CROP) were conducted on a library of electronically diverse *para*-substituted 2-phenyl-2-oxazolines. Polymerisations were conducted under microwave irradiation and monitored by ^{1}H NMR spectroscopy to elucidate kinetic parameters for both homo- and co-polymerisations. The inclusion of electron donating substituents in the *para*-position led to decreases in the rates of homopolymerisation compared to an unsubstituted 2-phenyl-2-oxazoline. Conversely, in copolymerisations, monomers containing electron donating substituents were incorporated at a higher rate than 2-phenyl-2-oxazoline, with the inverse effect observed with monomers displaying electron withdrawing substituents. The reactivity ratios of four representative monomer combinations were then determined using ^{1}H NMR spectroscopy and are consistent with a proposed model where copolymerisation kinetics are dictated largely by the relative nucleophilicity of the monomer.

Introduction

The cationic ring opening polymerisation (CROP) of 2-oxazolines offers access to well-defined macromolecules with a high degree of control over the structural features, and resultant properties, of the polymer. Since the first reports of CROP of 2-oxazolines in the 1960s,[1–4] a diverse range of functional polymers have been reported, with applications including packaging materials,[5] as surfactants,[6] and in biomaterials.[7] For example, block copolymers containing 2-oxazolines have been designed for solution self-assembly,[8] enabling transport of cargo including hydrophobic drugs.[9–12] In recent years, poly(2-oxazoline)s have been increasingly perceived as an alternative to PEG based polymers in biomedical applications,[13] as peptidomimetic materials that offer enhanced antibiofouling performance[14] and lower cytotoxicity.[15]

The increasing adoption of rapid microwave-assisted CROP[16–19] has opened the door to the generation of structurally diverse libraries of poly(oxazoline)s,[20] enabling the investigation of structure–property relationships.[21] Functionality can be introduced into poly(oxazoline) scaffolds at chain termini through choice of initiating and terminating agents,[22,23] or by introducing pendant functionality through selection of the 2-oxazoline monomer,[21] enabling convenient

tuning of the properties of the resultant polymers. 2-Oxazolines can be easily accessed from a variety of starting materials including aldehydes,[24] nitriles[25] and carboxylic acids,[26] enabling the preparation of a diverse range of functional macromolecules. The introduction of additional functionality in this manner can allow for the programming of polymer self-assembly, inclusion of temperature-[27] or pH-[28] responsive characteristics and tuning of polymer properties including viscoelasticity[29] and mechanical strength.[30] Modification of the 2-oxazoline core, however, can result in significant effects towards the kinetics of polymerisation,[31–33] as a consequence of differences in the stability of the propagating carbocation intermediate. In copolymerisations, the effect of differing monomer reactivity must also be considered. These differences in reactivity can be exploited to dictate the properties of the resultant polymer during synthesis. For example, the copolymerisation of 2-nonyl-2-oxazoline and 2-ethyl-2-oxazoline has been shown to yield random copolymers, whilst the replacement of 2-ethyl-2-oxazoline with 2-methyl-2-oxazoline leads to gradient copolymers.[34] Understanding the kinetics of copolymerisation is therefore critical to the preparation of complex polymer amphiphiles in one-pot approaches,[35] streamlining the synthesis of new functional materials.

Previous studies have suggested that the electron donating capability of a substituent can dramatically impact the rate of CROP of aryl oxazolines,[16,31] with electron donating substituents observed to decrease the rate of polymerisation, through stabilisation of the propagating carbocation. Schubert and co-workers have previously demonstrated this phenomenon using a set of mono- and di-fluorinated 2-phenyl-2-oxazolines, with

2-phenyl-2-oxazoline observed to polymerise more rapidly than the corresponding *para*-fluoro derivative. This observation suggests that the mesomeric donating effect of the fluorine substituent increases the electron density on the phenyl ring stabilising the propagating cation and thus lowers the rate of propagation.[33] A similar decrease in rate of polymerisation was observed by Saegusa and coworkers when studying the polymerisation of methyl- and methoxy- substituted 2-phenyl-2-oxazolines.[31] In some cases, it is difficult to quantitatively compare the findings of kinetic studies due to the range of reaction conditions employed, including differences in choice of solvents, initiators, reaction temperatures and concentrations.[36] This variation makes it difficult to quantitatively evaluate or predict the impact of factors such as electronics and sterics on the kinetics of polymerisation. This study aims to address how substituent effects alter the homopolymerisation and copolymerisation kinetics of a range of *para*-substituted 2-phenyl-2-oxazolines under set reaction conditions. We have therefore conducted kinetic studies across an electronically diverse library of oxazoline monomers with consistent polymerisation conditions, to allow for direct quantitative comparison of electronic effects.

Fig. 1 (i) Preparation of 2-phenyl-2-oxazolines by direct oxidative conversion from functionalised benzaldehydes.[23] (ii) A selection of *para*-substituted 2-phenyl-2-oxazolines prepared in this study.

Results and discussion

Homopolymerisations of *para*-substituted 2-phenyl-2-oxazolines

A representative series of *para*-substituted 2-phenyl-2-oxazolines was synthesised through reaction of the corresponding benzaldehydes with 2-aminoethanol in the presence of molecular iodine and potassium carbonate (Fig. 1; **1–10**),[24] with yields ranging between 46–75%. This synthetic strategy allowed for rapid generation of a diverse selection of monomers, featuring substituents with electron-donating or electron-withdrawing character through simple selection of the starting benzaldehyde.

Monomers **1–10** were subjected to microwave-assisted homopolymerisation *via* a method adapted from Sinnwell and Ritter,[37] using methyl *para*-toluenesulfonate as initiator (Table 1, 4 M monomer, 100 eq.). The kinetics of polymerisation were investigated by quenching polymerisations at different time points, and quantifying consumption of monomer using ^{1}H NMR spectroscopy, through integral analysis of signals corresponding to the hydrogens on positions 4 and 5 of the oxazoline ring (Fig. 2), compared to the hydrogens present in the solvent (DMF). In all cases, the polymerisations were observed to obey first-order kinetics (ESI, Section 1.4†).

Polymerisation of 2-phenyl-2-oxazoline monomer **1** was found to display $k_{obs} = 1.20 \times 10^{-3}$ s^{-1} (Table 1). Electron donating substituents, as defined by their Hammett parameters,[38] are represented in our palette of monomers by methoxy- (**2**), *tert*-butyl- (**3**) and methyl- (**4**) substituted 2-phenyl-2-oxazolines. The rate constants for homopolymerisation of these monomers were found to be at least an order of magnitude smaller than that of **1**, with $k_{obs} \sim 10^{-4}$–10^{-5} s^{-1}

(Table 1). This effect can be rationalised through stabilisation of the propagating carbocation through electron donation, which in turn lowers its susceptibility to nucleophilic attack, thus decreasing the rate of propagation.[21]

The presence of strongly electron withdrawing substituents such as nitro- (**10**), conversely, are postulated to destabilise the propagating carbocation, increasing its susceptibility to nucleophilic attack. Homopolymerisation of **10** was demonstrated to proceed with $k_{obs} = 2.50 \times 10^{-3}$ s^{-1} (Table 1), supporting this hypothesis. It was noted, however that a similar enhancement in rate was not observed during homopolymerisation of **9** (Table 1), which displays a more weakly electron withdrawing cyano-substituent. Halogenated 2-phenyl-2-oxazolines **5–8** were all observed to polymerise at a slower rate than **1**, with $k_{obs} \sim 10^{-4}$ s^{-1} (Table 1).

Whilst the incorporation of a *para*-halogen results in an inductive withdrawal of electron density it also provides a positive mesomeric effect, thus stabilising the propagating carbocation resulting in a slower rate of polymerisation. Gel permeation chromatography (GPC) analysis, where possible, (Table 1) revealed a range of dispersities between 1.1 and 1.5, suggesting that polymerisations proceeded with a degree of control. The M_n and M_w values obtained through GPC analysis were lower than would be predicted based on theoretical molecular weights and ^{1}H NMR spectroscopic analysis, consistent with previous reports,[39,40] reflecting differences in hydrodynamic volume between poly(oxazolines) and poly(methyl methacrylate) standards used for calibration.

Table 1 Summary of kinetic analysis and structural characterisation for homopolymerisations of **1–10**

Polymer	Monomer	k_{obs} (× 10^{-3} s^{-1})	DP[a]	M_n[a] (g mol^{-1})	M_n[b] (g mol^{-1})	M_w[b] (g mol^{-1})	Đ[b]
P1	**1**	1.20	83	12 200	2700	5400	1.2
P2	**2**	0.04	25	4 460	nd	nd	nd
P3	**3**	0.40	70	14 200	5300	6900	1.3
P4	**4**	0.40	79	12 700	4 100	5 800	1.5
P5	**5**	0.40	68	11 300	4200	6000	1.3
P6[c]	**6**	0.60	95	25 900	2500	2600	1.2
P7	**7**	0.40	47	8700	2700	3200	1.2
P8[c]	**8**	0.40	82	18 600	nd	nd	nd
P9[c]	**9**	0.20	68	11 700	nd	nd	nd
P10	**10**	2.50	35	6700	2500	3000	1.2

[a] Determined by ^{1}H NMR spectroscopy. [b] Determined by gel permeation chromatography (GPC) analysis in DMF + 1 g L^{-1} LiBr, 50 °C, 0.6 mL min^{-1}, calibrated using near monodisperse poly(methylmethacrylate) standards. [c] To the best of our knowledge, this report is the first to describe polymerisation of these monomers.
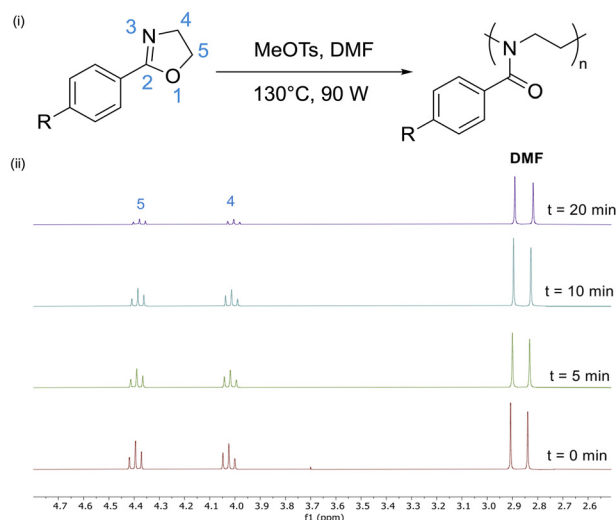
Fig. 2 (i) CROP of *para*-substituted 2-phenyl-2-oxazolines. (ii) ^{1}H NMR spectra (400 MHz, CDCl₃) acquired during polymerisation of **1**, showing the monomer depletion over time.

Fig. 3 Hammett plot for the homopolymerisations of *para*-substituted 2-phenyl-2-oxazolines **1–10**.

To further probe the impact of the electronic effects of substituents, a Hammett plot[38,41] was constructed (Fig. 3) demonstrating an overall correlation between Hammett substituent coefficient and measured rate constant. The most positive Hammett substituent constant, denoting the strongly electron withdrawing nature of the group, is presented by **10**, which displays the fastest rate of homopolymerisation. The opposite effect is observed in 2-phenyl-2-oxazolines with the most strongly electron donating substituents and most negative Hammett coefficients: methoxy-(**2**) and *tert*-butyl-(**3**), which display the slowest rates of homopolymerisation. The correlation observed in the Hammett plot evidences the impact of the *para*-substituent on the stability of the propagating carbocation, and consequently the rate of homopolymerisation. It is notable that the rate of homopolymerisation of **1** was greater than would be predicted based on the overall trend, resulting in the line of best fit not dissecting the origin, contrary to observations made by Saegusa and coworkers,[31] who con-structed a Hammett plot using a subset of the monomers explored here, under thermal activation. The higher than anticipated rate of homopolymerisation of **1** is, however, in line with observations made by Schubert and coworkers, whereby the *para*-substituted fluorinated monomer **5** displayed a slower rate of homopolymerisation under microwave irradiation than **1**, an observation that would not be predicted based upon Hammett parameters.[33] Other notable deviations from the line of best fit correspond to monomers **2** (*p*-OMe) and **9** (*p*-CN). These substituents exert a negative inductive effect, but a positive resonance effect, whereby electron density can be donated into the π-system, which is only partially accounted for using the Hammett σ constant.[41]

Copolymerisations of *para*-substituted 2-phenyl-2-oxazolines with unsubstituted 2-phenyl-2-oxazoline 1

Having noted differences in relative reactivities of **1–10**, we next wished to explore their copolymerisations. Four representative monomers were selected for copolymerisation with **1**, displaying methoxy-(**2**), methyl-(**4**), bromo-(**8**) and nitro-(**10**) substituents, allowing for the investigation of the effects of

electron donation and withdrawal through resonance and induction.

An alternative method of analysis was required to determine the composition of the reaction mixture during copolymerisations, as signals corresponding to protons at positions 4 and 5 (Fig. 4(i)) of the oxazoline monomers were observed to overlap in ^{1}H NMR spectra acquired during copolymerisations. In addition, the ^{1}H NMR signals corresponding to aryl protons of monomers were observed to be distinct, but overlapped with the corresponding signals from the polymer. It was therefore necessary to suppress macromolecular resonances to enable monomer quantification by ^{1}H NMR spectroscopy. This suppression is typically achieved by exploiting the differences in spin–spin relaxation (characterised by the T_2 constant) between large and small entities, as large entities have shorter T_2 (broader signals) than small ones (sharper signals).[42] The Carr–Purcell–Meiboom–Gill (CPMG)[43] T_2 filter is most commonly used to supress signals corresponding to macromolecules, however, CPMG pulse sequences are energy intensive, and require refocussing times that may damage the spectrometer if used for more than 100 ms, depending on hardware specifications. In cases such as ours, the differences in T_2 are the smallest at the beginning of the reaction, as the

molecular weight of the polymer is small. To differentiate between the signals of the incipient polymers and those of small molecules, the T_2 filter time must be extended beyond the safe limits of the CPMG pulse sequence. To solve this problem, we adopted the approach of Morris and coworkers,[44] who proved that CPMG filter times can be greatly extended by introducing planar mixing in the form of a perfect echo. Using this approach, dubbed PROJECT, we managed to use T_2 filters of 350 ms, filter times that are long enough to suppress the polymer signals at all stages of the reaction. Care must be taken when using T_2 filters to monitor polymerisations because of the fact that the T_2 of all signals will decrease if the viscosity of the sample increases.[45] To compensate for this effect, samples were taken from the reaction vessel and diluted before analysis, signals were normalised to a known concentration of reference molecule (DMF) and T_2 spectra were overlaid to check for variation in the linewidth of the signals, as the linewidth is inversely proportional to T_2. This method allowed for the resolution of resonances corresponding to small molecules and polymers.

In the copolymerisation of **1** with *para*-OMe substituted **2**, it was observed that **2** was incorporated within the polymer at a faster rate (Fig. 5(i)), consistent with its increased nucleophilicity. A similar, though less pronounced effect was observed during copolymerisation of **1** with methyl-substituted **4** (Fig. 5(ii)). Similarly, during copolymerisation of **1** with bromo-substituted **8**, the more electron rich **1** was incorporated more rapidly (Fig. 5(iii)). Whilst nitro-substituted **10** had been observed to display the fastest rate of homopolymerisation (Table 1), a feature attributed to destabilisation of the propagating cation, during copolymerisation it was observed to display a limited rate of incorporation, likely as a consequence of its decreased nucleophilicity compared to **1**. Other literature reports support this reversal in the monomer reactivity across homopolymerisations and copolymerisations for oxazolines and oxazines,[35,46] where the oxazine monomer is consumed in preference to the oxazoline. The effect can be explained by the increased nucleophilicity of the oxazine nitrogen compared to the oxazoline nitrogen.

To further investigate the kinetics of copolymerisation, reactivity ratios were determined using both the Mayo–Lewis and Fineman–Ross models (Table 2 and ESI Section 1.6–1.7†).[47] These analysis methods require the quantitative determination of monomer consumption at low conversion. Under these conditions it was judged that monomer consumption could be directly determined by integral analysis of signals corresponding to aryl protons, as no macromolecular resonances could be observed.[47,48] Polymerisations were conducted at various feed ratios for 2 min without sampling to ensure sufficiently low monomer conversion to prevent changes in effective monomer concentration.

Copolymerisation of **1** and **2** resulted in an r_A value of 0.3, suggesting propagating chains terminated with **1** favour cross-propagation, and r_B 1.3, indicating a preference for self-propagation of chains terminated with **2**. This observation suggests that the increased nucleophilicity of **2** exerts a greater effect on
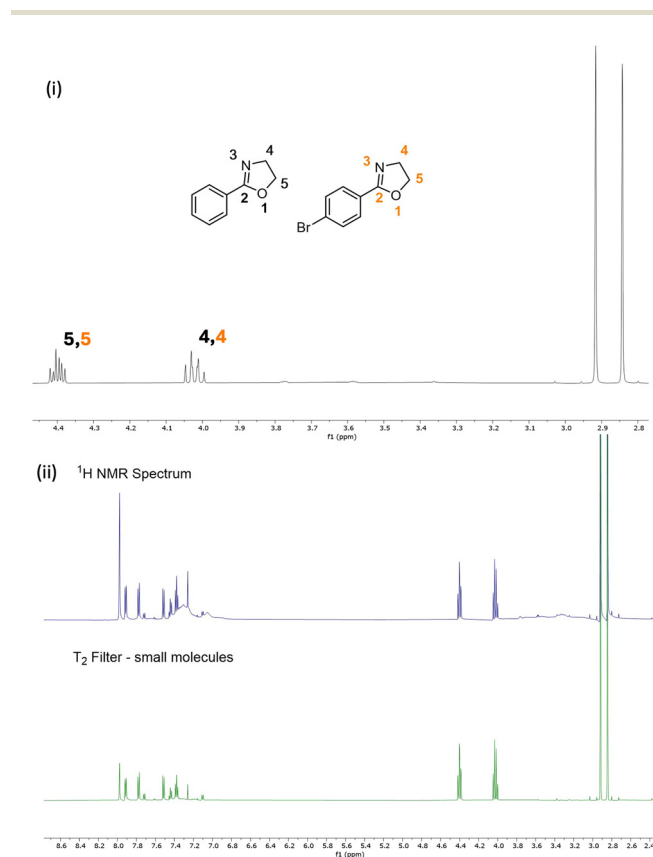

Fig. 4 (i) Partial ^{1}H NMR spectrum (400 MHz, CDCl$_3$) of copolymerisation of **1** and **8**, showing overlap of the signals corresponding to monomers. (ii) ^{1}H NMR spectrum (400 MHz, CDCl$_3$) of the same reaction mixture with T_2 filter applied.
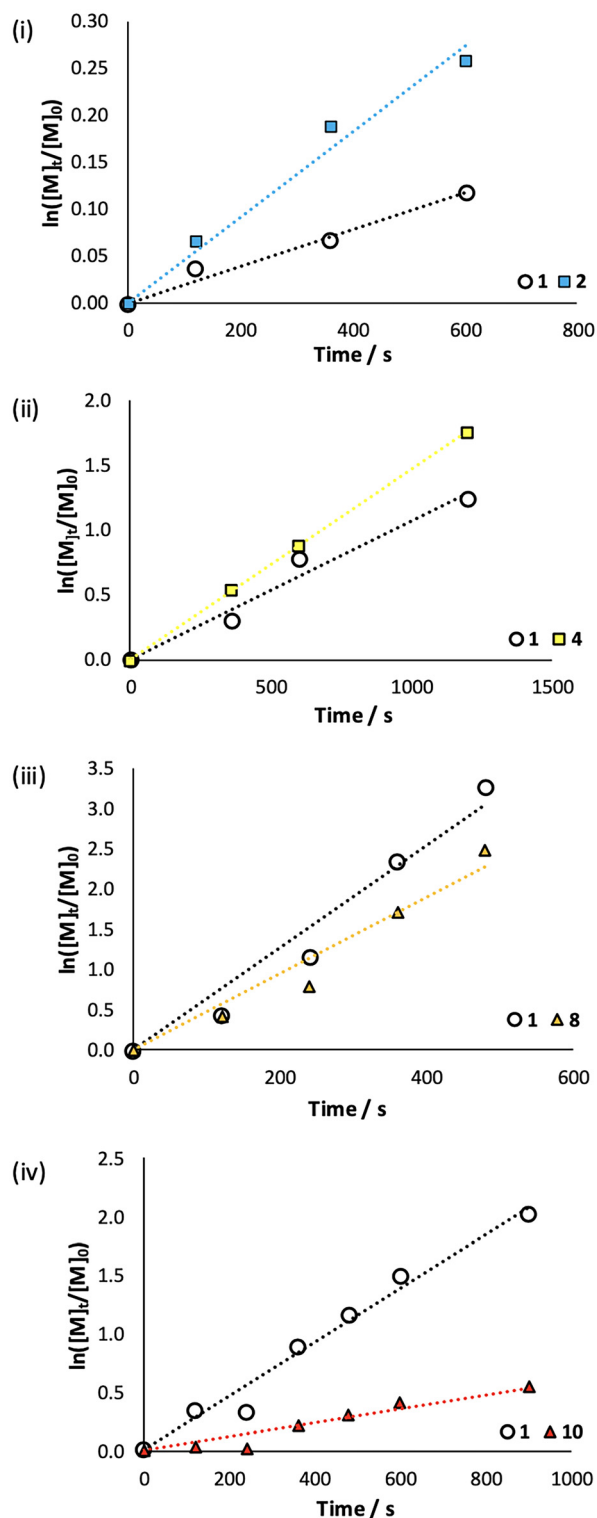
Fig. 5 Analysis of monomer consumption during copolymerisations of **1** with (i) **2**; (ii) **4**; (iii) **8** (iv) **10**. 4 M total monomer concentration (100 eq.), MeOTs, DMF, 90 W, 130 °C.

Table 2 Reactivity ratios for the copolymerisation of **1** with representative *para*-substituted 2-phenyl-2-oxazolines using both the Mayo−Lewis and Fineman−Ross methods of analysis

		Mayo–Lewis		Fineman–Ross	
Monomer A	Monomer B	r_A	r_B	r_A	r_B
1	**2**	0.3	1.3	0.3	1.3
1	**4**	1.7	3.2	1.7	3.2
1	**8**	1.4	0.9	1.5	1.1
1	**10**	nd	Nd	1.5	0.0^a

^{a} An r_B value of −0.4 was determined (ESI Section 1.7†). The Fineman–Ross model suggests that any negative values can be approximated to 0, representative of an extremely slow rate of uptake.

display a preference for self-propagation, which is more pronounced in the case of **4** (r_B 3.2; r_A 1.7). Within this combination of monomers, the inductive electron donation supplied by the methyl substituent in **4** would be expected to contribute less to both monomer nucleophilicity and stabilisation of the propagating carbocation than in the case of **1** and **2**.

In the case of copolymerisation of **1** and **8**, **1** displayed some preference for self-propagation (r_A ~1.5), consistent with its increased nucleophilicity, while **8** displayed no significant preference for self- or cross-propagation (r_B 0.9/1.1), suggesting that the halogen substituent exerts limited stabilising/destabilising influence on the propagating carbocation. A more pronounced effect was observed during the copolymerisation of **1** and **10**, where **1** was observed to display a preference for self-propagation (r_A 1.5), while an r_B value of 0 was obtained for **10**, suggesting negligible self-propagation. This behaviour is in line with our observations of limited consumption of **10** during copolymerisation with **1** (Fig. 5(iv)), and the decreased nucleophilicity of **10** on account of the electron withdrawing effect of the nitro-substituent.

Overall, these observations are consistent with a model where copolymerisation kinetics are dictated largely by the relative nucleophilicity of the monomer, with effects of stabilisation or destabilisation of the propagating chain contributing to a lesser extent.

Conclusion

The electron withdrawing or donating capability of a *para*-substituent on a 2-phenyl-2-oxazoline monomer has a significant impact on kinetics of homopolymerisation, with an electron withdrawing nitro-substituent observed to greatly increase the rate of polymerisation. Conversely, electron donating substituents were observed to lead to a decrease in the rate of polymerisation with respect to the unsubstituted monomer, presumably due to stabilisation of the propagating carbocation.

The copolymerisation kinetics of 2-phenyl-2-oxazoline **1** with a selection of *para*-substituted 2-phenyl-2-oxazolines were studied using the PROJECT T_2 filter approach[44,49] to enable determination of monomer consumption during copolymeri-

copolymerisation kinetics than the stabilisation offered to the propagating chain by the electron-donating methoxy substituent. During copolymerisation of **1** and **4**, both monomers

sation. 2-Phenyl-2-oxazolines with electron donating substituents displayed increased rates of polymerisation compared to **1**, on account of increased nucleophilicity of these monomers. The opposite effect was observed for the copolymerisation of **1** with the nitro-substituted monomer **10**, as a consequence of the decreased nucleophilicity of this monomer. Reactivity ratios were determined using the Fineman–Ross and Mayo–Lewis methods, and suggested that the incorporation of the next monomer unit during copolymerisation is largely dictated by the relative nucleophilicity of the monomer, with substituent effects on the stability of the propagating chain observed to contribute to a lesser extent.

Author contributions

CMS: investigation, methodology, data curation, formal analysis, visualisation, writing – original draft. LAS: methodology, data curation, formal analysis, writing – review and editing. JAA: investigation, methodology, data curation, writing – review and editing. WDGB: conceptualisation, supervision, funding acquisition, resources, validation, visualisation, writing – review and editing. CSM: conceptualisation, supervision, funding acquisition, resources, validation, visualisation, writing – review and editing.

Conflicts of interest

There are no conflicts to declare.

Data availability

Data supporting this article has been supplied within the ESI.†

Acknowledgements

References

1 D. A. Tomalia and D. P. Sheetz, *J. Polym. Sci., Part A: Polym. Chem.*, 1966, **4**, 2253–2265.

2 W. Seeliger, E. Aufderhaar, W. Diepers, R. Feinauer, R. Nehring, W. Thier and H. Hellmann, *Angew. Chem., Int. Ed. Engl.*, 1966, **5**, 875–888.

3 T. Kagiya, S. Narisawa, T. Maeda and K. Fukui, *J. Polym. Sci., Part B: Polym. Phys.*, 1966, **4**, 441–445.

4 T. G. Bassiri, A. Levy and M. Litt, *J. Polym. Sci., Part B: Polym. Phys.*, 1967, **5**, 871–879.

5 R. Konradi, C. Acikgoz and M. Textor, *Macromol. Rapid Commun.*, 2012, **33**, 1663–1676.

6 S. Kobayashi, T. Igarashi, Y. Moriuchi and T. Saegusa, *Macromolecules*, 1986, **19**, 535–541.

7 S. Nemati Mahand, S. Aliakbarzadeh, A. Moghaddam, A. Salehi Moghaddam, B. Kruppke, M. Nasrollahzadeh and H. A. Khonakdar, *Eur. Polym. J.*, 2022, **178**, 111484.

8 S. C. Lee, Y. Chang, J.-S. Yoon, C. Kim, I. C. Kwon, Y.-H. Kim and S. Y. Jeong, *Macromolecules*, 1999, **32**, 1847–1852.

9 K. M. Huh, S. C. Lee, Y. W. Cho, J. Lee, J. H. Jeong and K. Park, *J. Controlled Release*, 2005, **101**, 59–68.

10 C.-H. Wang, C.-H. Wang and G.-H. Hsiue, *J. Controlled Release*, 2005, **108**, 140–149.

11 C.-H. Wang, W.-T. Wang and G.-H. Hsiue, *Biomaterials*, 2009, **30**, 3352–3358.

12 T. X. Viegas, M. D. Bentley, J. M. Harris, Z. Fang, K. Yoon, *et al.*, *Bioconjugate Chem.*, 2011, **22**, 976–986.

13 S. Lowe, N. M. O'Brien-Simpson and L. A. Connal, *Polym. Chem.*, 2015, **6**, 198–212.

14 B. Pidhatika, M. Rodenstein, Y. Chen, E. Rakhmatullina, A. Mühlebach, C. Acikgöz, M. Textor and R. Konradi, *Biointerphases*, 2012, **7**, 1.

15 R. Luxenhofer, G. Sahay, A. Schulz, D. Alakhova, T. K. Bronich, R. Jordan and A. V. Kabanov, *J. Controlled Release*, 2011, **153**, 73–82.

16 R. Hoogenboom, M. A. M. Leenen, F. Wiesbrock and U. S. Schubert, *Macromol. Rapid Commun.*, 2005, **26**, 1773–1778.

17 K. P. Luef, R. Hoogenboom, U. S. Schubert and F. Wiesbrock, in *Microwave-assisted Polymer Synthesis*, ed. R. Hoogenboom, U. S. Schubert and F. Wiesbrock, Springer International Publishing, Cham, 2016, pp. 183–208.

18 F. Wiesbrock, R. Hoogenboom, C. H. Abeln and U. S. Schubert, *Macromol. Rapid Commun.*, 2004, **25**, 1895–1899.

19 K. Kempe, C. R. Becer and U. S. Schubert, *Macromolecules*, 2011, **44**, 5825–5842.

20 R. Hoogenboom, *Macromol. Chem. Phys.*, 2007, **208**, 18–25.

21 M. Glassner, M. Vergaelen and R. Hoogenboom, *Polym. Int.*, 2018, **67**, 32–45.

22 A. Lusina, T. Nazim and M. Cegłowski, *Polymers*, 2022, **14**, 640.

23 C. Giardi, V. Lapinte, C. Charnay and J. J. Robin, *React. Funct. Polym.*, 2009, **69**, 643–649.

24 M. Ishihara and H. Togo, *Tetrahedron*, 2007, **63**, 1474–1480.

25 H. Witte and W. Seeliger, *Justus Liebigs Ann. Chem.*, 1974, **1974**, 996–1009.

26 X. Huang, W. Zhao, D.-L. Chen, Y. Zhan, T. Zeng, H. Jin and B. Peng, *Chem. Commun.*, 2019, **55**, 2070–2073.

27 R. Obeid, E. Maltseva, A. F. Thünemann, F. Tanaka and F. M. Winnik, *Macromolecules*, 2009, **42**, 2204–2214.

28 C. Kim, S. C. Lee, J. H. Shin, J.-S. Yoon, I. C. Kwon and S. Y. Jeong, *Macromolecules*, 2000, **33**, 7448–7452.

29 L. Hahn, M. Maier, P. Stahlhut, M. Beudert, V. Flegler, *et al.*, *ACS Appl. Mater. Interfaces*, 2020, **12**, 12445–12456.

30 E. F. J. Rettler, J. M. Kranenburg, H. M. L. Lambermont-Thijs, R. Hoogenboom and U. S. Schubert, *Macromol. Chem. Phys.*, 2010, **211**, 2443–2448.

31 S. Kobayashi, T. Tokuzawa and T. Saegusa, *Macromolecules*, 1982, **15**, 707–710.

32 K. Kempe, M. Lobert, R. Hoogenboom and U. S. Schubert, *J. Polym. Sci., Part A-1: Polym. Chem.*, 2009, **47**, 3829–3838.

33 M. Lobert, U. Köhn, R. Hoogenboom and U. S. Schubert, *Chem. Commun.*, 2008, 1458–1460.

34 R. Hoogenboom, M. W. M. Fijten, S. Wijnans, A. M. J. van den Berg, H. M. L. Thijs and U. S. Schubert, *J. Comb. Chem.*, 2006, **8**, 145–148.

35 O. Sedlacek, K. Lava, B. Verbraeken, S. Kasmi, B. G. De Geest and R. Hoogenboom, *J. Am. Chem. Soc.*, 2019, **141**, 9617–9622.

36 S. Abbrent, A. Mahun, M. D. Smrčková, L. Kobera, R. Konefał, P. Černoch, K. Dušek and J. Brus, *RSC Adv.*, 2021, **11**, 10468–10478.

37 S. Sinnwell and H. Ritter, *Macromol. Rapid Commun.*, 2005, **26**, 160–163.

38 L. P. Hammett, *J. Am. Chem. Soc.*, 1937, **59**, 96–103.

39 Z. Varanaraja, R. Terracciano, N. Hollingsworth, R. Green, J. Beament and C. R. Becer, *Macromolecules*, 2024, **57**, 5769–5779.

40 J. Kim, V. Beyer and C. R. Becer, *Macromolecules*, 2022, **55**, 10651–10661.

41 C. Hansch, A. Leo and R. W. Taft, *Chem. Rev.*, 1991, **91**, 165–195.

42 J. A. Aguilar, R. W. Adams, M. Nilsson and G. A. Morris, *J. Magn. Reson.*, 2014, **238**, 16–19.

43 S. Meiboom and D. Gill, *Rev. Sci. Instrum.*, 1958, **29**, 688–691.

44 J. A. Aguilar, M. Nilsson, G. Bodenhausen and G. A. Morris, *Chem. Commun.*, 2012, **48**, 811–813.

45 T. R. Nelson and S. M. Tung, *J. Magn. Reson. Imaging*, 1987, **5**, 189–199.

46 Z. Varanaraja, J. Kim and C. R. Becer, *Eur. Polym. J.*, 2021, **147**, 110299.

47 M. Fineman and S. D. Ross, *J. Polym. Sci.*, 1950, **5**, 259–262.

48 M. Concilio, R. G. Maset, L. P. Lemonche, V. Kontrimas, J.-I. Song, S. K. Rajendrakumar, F. Harrison, C. R. Becer and S. Perrier, *Adv. Healthcare Mater.*, 2023, **12**, 2301961.

49 M. Foroozandeh, G. A. Morris and M. Nilsson, *Chem. – Eur. J.*, 2018, **24**, 13988–14000.